Shining light on single-strand lesions caused by the chemotherapy drug bleomycin

DNA Repair 105 (2021) 103153

Contents lists available at ScienceDirect

DNA Repair

journal homepage: www.elsevier.com/locate/dnarepair

Shining light on single-strand lesions caused by the chemotherapy drug bleomycin

Vandana Singh [a,b,*], Pegah Johansson [b,c], Yii-Lih Lin [a], Ola Hammarsten [b,c], Fredrik Westerlund [a,*]

[a] Biology and Biological Engineering, Chalmers University of Technology, Gothenburg, Sweden
[b] Laboratory of Clinical Chemistry, Sahlgrenska University Hospital, Gothenburg, Sweden
[c] Department of Laboratory Medicine, Institute of Biomedicine, Sahlgrenska Academy at University of Gothenburg, Gothenburg, Sweden

ARTICLE INFO

Keywords:
Single molecule imaging
DNA damage
BER inhibition
Fluorescence microscopy
Single-strand breaks
Personalizing chemotherapy
Damage mechanism of drugs

ABSTRACT

Quantification of the DNA damage induced by chemotherapy in patient cells may aid in personalization of the dose used. However, assays to evaluate individual patient response to chemotherapy are not available today. Here, we present an assay that quantifies single-stranded lesions caused by the chemotherapeutic drug Bleomycin (BLM) in peripheral blood mononuclear cells (PBMCs) isolated from healthy individuals. We use base excision repair (BER) enzymes to process the DNA damage induced by BLM and then extend the processed sites with fluorescent nucleotides using a DNA polymerase. The fluorescent patches are quantified on single DNA molecules using fluorescence microscopy. Using the assay, we observe a significant variation in the *in vitro* induced BLM damage and its repair for different individuals. Treatment of the cells with the BER inhibitor CRT0044876 leads to a lower level of repair of BLM-induced damage, indicating the ability of the assay to detect a compromised DNA repair in patients. Overall, the data suggest that our assay could be used to sensitively detect the variation in BLM-induced DNA damage and repair in patients and can potentially be able to aid in personalizing patient doses.

1. Introduction

Chemotherapy drugs kill proliferating cancer cells by targeting DNA, RNA [1], enzymes [2] and proteins [3]. The drugs can be classified based on their ability to induce different forms of DNA damage, the most common being single-strand breaks (SSBs), double-strand breaks (DSBs) and DNA-protein crosslinks [4]. Some examples are crosslinking agents, such as cisplatin and carboplatin [5], alkylating agents, such as cyclophosphamide and busulfan [6] and oxidizing agents, such as bleomycin (BLM) [7].

Differences in individual normal tissue sensitivity results in variation in the severity of side effects and is a challenge to optimal dosing of chemotherapy. Factors like age, previous exposure to radiation or chemotherapy, gender, rate of metabolism of chemotherapy drugs and other genetic traits can affect the outcome of chemotherapy [8,9]. Despite the broad use of chemotherapy, there are no clinically available assays that can predict patient's hypersensitivity or resistance towards specific chemotherapy drugs.

BLM is a glycopeptide with antibiotic and anti-tumour properties [10]. It is used for treatment of cancers with various tissue origin such as testes, ovarian, cervical as well as Hodgkin's and non-Hodgkin's lymphomas [11]. BLM interacts with Fe(II) and O_2 to give a ternary complex that is responsible for its DNA cleaving activity [12]. BLM also complexes with divalent copper to form BLM:Cu(II) complexes [13]. However, there are conflicting reports regarding the DNA damaging potential of BLM:Cu(II) [14–16]. The main mechanism of DNA damage by BLM is oxidation at the C-4′ position on the DNA, leading to strand breaks with 1-base 5′-overhangs and with predominantly 3′-phosphoglycolate termini along with DSBs with blunt ends [17]. The repair of DNA lesions caused by BLM can be initiated by enzymes of the base excision repair (BER) pathway. An example is APE1, the human analogue of bacterial exonuclease III that is both an AP-endonuclease and a 3′ to 5′ exonuclease, which cleaves bulkier 3′ adducts, making DNA ends ready for downstream polymerization and ligation [18–20]. There are certain inhibitors of BER, such as CRT0044876 (CRT), that can selectively slowdown BER by directly inhibiting APE1 [21]. This is a

* Corresponding authors at: Biology and Biological Engineering, Chalmers University of Technology, Gothenburg, Sweden.
E-mail addresses: vsingh@chalmers.se (V. Singh), fredrikw@chalmers.se (F. Westerlund).

https://doi.org/10.1016/j.dnarep.2021.103153
Received 6 November 2020; Received in revised form 17 May 2021; Accepted 2 June 2021
Available online 10 June 2021

potential target in cancer therapy that can enhance the cytotoxicity of chemotherapy drugs in cancerous cells [22,23].

Assays for quantification of DNA damage include the comet assay [24], and immunoassays based on antibodies that recognize specific DNA-adducts [25,26]. The immunoassays can be very sensitive, but often only measure a specific type of DNA damage, like the 8-oxo-G adduct formed after oxidative damage [27,28]. In addition, very few specific antibodies are commercially available and cross reactivity of antibodies with DNA makes these assays less viable in clinical settings, where quantification of global levels of DNA damage is important [29].

Previously, UV, ethanol and hydrogen peroxide induced DNA damage has been quantified in various cell lines through single-DNA molecule imaging [30–32]. The method uses BER enzymes to initiate the DNA repair of the damaged bases *in vitro* and then the damage sites are labeled by fluorescent dNTPs using DNA polymerases [32–34]. Recently, the method has also been modified and used in fixed cells to measure DNA damage *in situ* where relative fluorescence intensity is measured [35]. However, DNA damage detection on the single molecule level can detect low levels of damage more sensitively and is compatible with optical DNA mapping [36]. The assay reports the number of lesions per DNA length and also allows DNA repair to be followed in real time. We have shown that the same assay can be extended to ionizing radiation and hyperthermia induced single strand DNA damage on PBMCs derived from healthy individuals [37].

In this work, we have further optimized this DNA damage assay for detecting BLM-induced DNA damage in patient derived cells. Human APE1 and the bacterial homologue Endo IV are important for detecting the DNA damage caused by BLM. We also demonstrate BER inhibition caused by the APE1 inhibitor CRT0044876, which we propose as a model for identifying individuals with defective DNA repair pathways. Future potential use of the assay ranges from predicting drug and dose outcomes for cancer patients, analysis of repair of SSBs caused by chemotherapy drugs for identifying sensitive patients, as well as elucidation of damage mechanisms of different chemotherapy drugs.

2. Materials and methods

2.1. Blood samples

Excess blood (EDTA tubes) from individuals with normal differential blood count were collected from the Hematology unit at the Clinical Chemistry laboratory at Sahlgrenska University Hospital.

2.2. Drug preparations

Stock solutions, 50 mM each, of BLM sulphate (Sigma-Aldrich and ThermoFisher), $FeSO_4{\cdot}6H_2O$ (Sigma-Aldrich), $Cu(NO_3)_2{\cdot}3H_2O$ (Sigma-Aldrich) were prepared in MQ water and stored at −80 °C. BLM sulphate (0.25 mM) and $FeSO_4{\cdot}6H_2O$ (0.25 mM) or $Cu(NO_3)_2{\cdot}3H_2O$ (0.25 mM) were mixed at a molar ratio of 1:1, followed by incubation at 37 °C for 30 min before treatment of PBMCs. A 50 mM CRT0044876 (EMD Millipore Corp. USA) stock solution was prepared in DMSO (SIGMA Life Science) and stored at −20 °C.

2.3. PBMCs preparation and treatment

Density centrifugation using Lymphoprep (Axis-Shield PoC AS, Oslo, Norway) was performed to prepare PBMCs according to the manufacturer's protocol. PBMCs were resuspended in RPMI 1640 prior to treatment according to the lymphocyte count for each individual (2.5×10^5 lymphocytes/ 400 μL), and treated with 3 μM BLM:Fe(II) (for repair kinetics) or left untreated for 1 h at 37 °C in repair. The cells were then resuspended in 1X Hanks' Balanced Salt Solution (HBSS) and centrifuged at 300 *g* for 5 min at 4 °C. For repair kinetics, the pelleted cells were resuspended in RPMI 1640 at 37 °C and harvested at time intervals ranging from 20 min to 90 min together with an untreated sample, as indicated in the figures. For the 0 min time point, aliquots were taken directly after treatment followed by DNA extraction.

For APE1 inhibition, PBMCs (2.5×10^5 cells/ 400 μL) were treated with CRT0044876 (200 μM) for 2 h at 37 °C prior to BLM:Fe(II)(3 μM) treatment for 1 h at 37 °C. One aliquot was harvested at 0 min. 1X HBSS was added and the cells were centrifuged for 5 min at 300 *g* at 4 °C. The cells were resuspended in RPMI and incubated for 90 min at 37 °C before harvest. For further APE1 inhibition, samples containing CRT0044876 and CRT:BLM:Fe(II) were resuspended in RPMI 1640 at a final concentration of 200 μM CRT0044876 for 90 min.

2.4. DNA extraction

GenElute-Mammalian Genomic DNA Miniprep Kit (Sigma-Aldrich) was used for DNA extraction according to the manufacturers' protocol, using wide bore pipette tips throughout the procedure to minimize shear-induced fragmentation of the DNA.

2.5. Labeling of damage sites

The labeling of the damage sites was carried out as described previously with a few modifications [31]. Firstly, 100 ng of DNA was incubated with an enzyme cocktail containing APE1 (2.5 U), FpG (2.5 U), Endo III (2.5 U), Endo IV (2.5 U), Endo VIII (2.5 U) and UDG (2.5 U) in 1X CutSmart Buffer (New England BioLabs (NEB)) for 1 h at 37 °C unless otherwise noted. In some experiments, single enzymes, or a combination of EndoIV and APE1, were used as indicated in each figure. All enzymes were purchased from NEB. The fluorescent labeling of the damage sites was performed with dNTPs (Sigma-Aldrich) (1 μM of dATP, dGTP, dCTP, 0.25 μM dTTP and 0.25 μM Aminoallyl-dUTP-ATTO-647 N (Jena Bioscience) and DNA polymerase 1 (1.25 U) in 1X NEBuffer 2 (NEB) for 1 h at 20 °C. The reaction was terminated with 2.5 μL of 0.25 M EDTA (Sigma-Aldrich).

2.6. Silanization of coverslips

The silanization of glass coverslips was adapted from Wei et al. [38]. Briefly, 22 × 22 mm, No. 1 coverslips (MARIENFELD laboratory glassware) were submerged in a mixture of 1% (3-aminopropyl) triethoxysilane (APTES, Sigma), 1% allyltrimethoxysilane (ATMS, Sigma), and acetone, and were silanized for 1 h. The coated coverslips were rinsed with an acetone:water solution (2:1 v/v) and dried by air purging. The air-dried coverslips were stored in airtight petri dishes and used within a week.

2.7. Staining of DNA backbone and imaging

The fluorescently labeled human genomic DNA and lambda DNA (7 μL/sample) was stained with 320 nM YOYO-1 (Invitrogen) in 0.5 × TBE, supplemented with 1 μL of β-mercaptoethanol (BME, Sigma-Aldrich) at a final volume of 50 μL. Each sample (3.8 μL) was then extended on the silanized 22 × 22 mm^2 coverslips by placing the solution at the interface of an activated coverslip and a clean microscopy slide (Thermo SCIENTIFIC, MENZEL-GLÄSER). The extended DNA molecules were imaged with a fluorescence microscope (Zeiss Observer.Z1) and an Andor iXON Ultra EMCCD camera. Band-pass excitation filters (475/40 and 640/30) and bandpass emission filters (530/50 and 690/50) were used for YOYO-1 and Aminoallyl-dUTP-ATTO-647 N, respectively. An EM gain setting of 100 and exposure times of 30 ms and 500 ms were used for YOYO-1 and Aminoallyl-dUTP-ATTO-647 N, respectively.

2.8. Data analysis

A custom-made software was used to analyze the data as described previously [39]. The total DNA length in each image was estimated in pixels and the total number of Aminoallyl-dUTP-ATTO-647N dots

(patches) along each single DNA molecule was counted. Then the number of Aminoallyl-dUTP-ATTO-647N-labeled sites was calculated as dots/pixel. Two or more damage sites positioned within the diffraction limit that could not be resolved were counted as one dot. The software was programmed to exclude overlapping DNA strands from quantification. Lambda DNA (48502 bp) was extended on the activated coverslip in the same buffer conditions as the reaction mixture to estimate the DNA length per pixel to 1 μm = ~3000 bp (Supplementary Table 1). This was then used to convert pixels to DNA length (1 pixel=0.129 μm). The data were then presented as dots/Mbp as follows:

Damage detected (DD, dots/Mbp) = total number of sites detected per DNA length

2.9. Statistics

The experiments were performed in technical triplicates unless otherwise noted, and differences between the groups were assessed by ANOVA analysis (Tukey's post-hoc test) with significance at $p < 0.05$ (*** *represents* $p < 0.001$, * $p < 0.05$). At least a total of 20 Mbp of DNA was analyzed per sample.

3. Results

3.1. Detection of DNA damage caused by BLM

The DNA damage detection assay was optimized to assess the amount of single-strand DNA lesions induced by BLM. The DNA from BLM-treated PBMCs was extracted and the labeling of the DNA was performed in a two-step procedure, as schematically shown in Fig. 1A-B (details in Methods). In the first step a cocktail of repair enzymes was used to process the damaged DNA ends to make them accessible for post-processing by a DNA polymerase. The second step consisted of using a mix of dNTPs containing one fluorescent analogue and DNA polymerase 1, leading to formation of DNA labeled with fluorescent spots. The backbone of the labeled DNA molecules was stained with the fluorescent dye YOYO-1, and the DNA molecules were stretched on functionalized coverslips. Images were acquired using a fluorescence microscope and data quantification was performed giving the detected damage (DD) values as dots/MBp (see Methods).

3.2. Detection of BLM dose response in PBMCs

To optimize the assay conditions, the cells were treated with increasing concentrations of BLM, BLM:Fe(II), BLM:Cu(II), Fe(II) and Cu (II) and the single-strand DNA lesions were quantified using our assay (Figs. 2 and S1). The damage detected increased significantly at

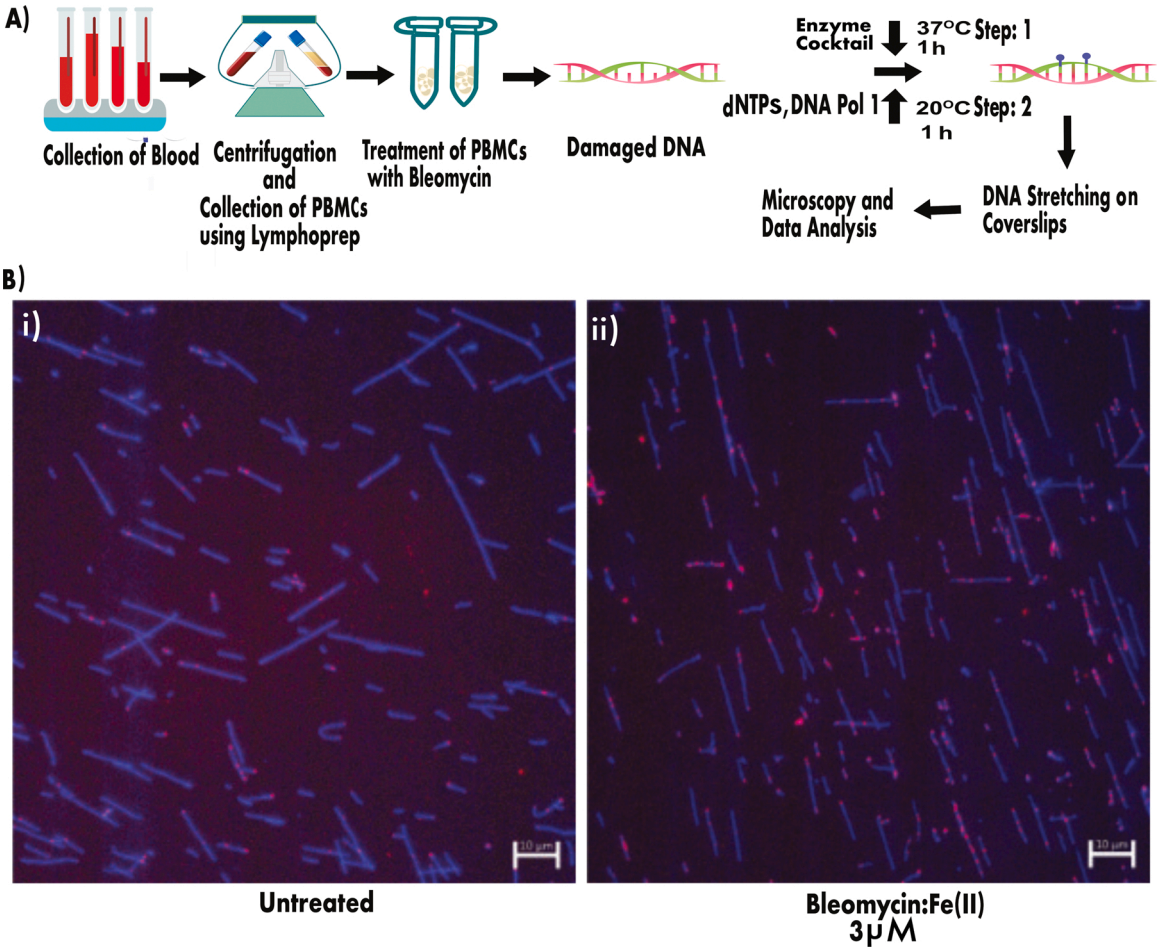

Fig. 1. A. Schematic of the steps involved in PBMCs isolation and labeling of BLM-induced damage. The labeling was performed in two steps; first the BER enzymes are used to remove the DNA damages and make the sites ready for polymerization, and second these sites are labeled using DNA polymerase 1 and dNTPs having one fluorescent analogue Aminoallyl-dUTP-ATTO-647 N (see Methods section). After labeling, the DNA is stretched in-between a silane-functionalized coverslip and a glass slide, followed by image acquisition. **B**. Representative images of (i) untreated and (ii) BLM:Fe(II)(3 μM) treated samples. The magenta dots are the Aminoallyl-dUTP-ATTO-647 N patches and blue is the YOYO-1 stained DNA. Scale bar =10 μm.

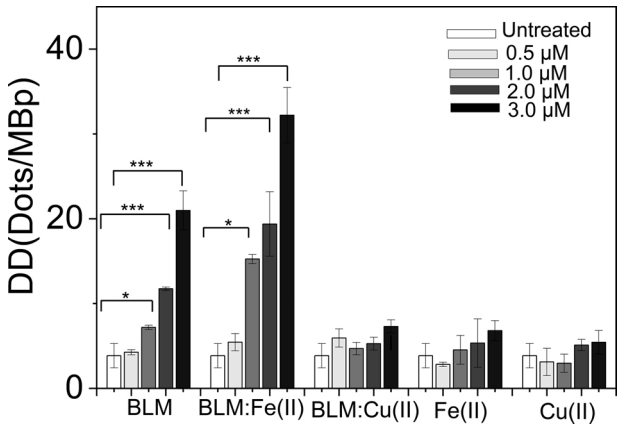

Fig. 2. Detected DNA damage in PBMCs collected from pooled blood (five healthy individuals) exposed to increasing concentrations (from 0 to 3 μM) of BLM, BLM:Fe(II), BLM:Cu(II), Fe(II) and Cu(II), detected using the whole enzyme cocktail. Error bars indicate the standard deviation calculated from technical triplicates.

increasing concentrations of BLM alone and BLM:Fe(II), but not BLM:Cu (II), Cu(II) alone, or Fe(II) alone. The BLM induced damage was higher in the presence of Fe(II) for all treatment concentrations. Therefore BLM: Fe(II) was used for the rest of this study.

3.3. Detection of BLM:Fe(II)-induced DNA damage using single enzymes

In the previous section we used a cocktail of repair enzymes to detect BLM and BLM:Fe(II) induced DNA damage in blood pooled from five individuals. To determine the relative contribution of each enzyme to damage detection, we next studied single enzymes. We observed a significant increase in detected damage with Endo IV (~6.0 times), and APE1 (~4.2 times), with respect to the untreated samples (Figs. 3A and S2). On the other hand, FpG, Endo III, Endo VIII, UDG did not result in a significant increase in detected damage when used alone. Next, we compared the amount of damage detected with a combination of Endo IV and APE1 to a cocktail containing all enzymes, again in pooled blood. Interestingly, at the lower BLM concentration (2 μM), Endo IV and APE1 identified the same number of damage sites as the whole cocktail, while at the higher concentration (3 μM), a significantly higher level of damage was detected with the cocktail (Fig. 3B). As the cocktail detected more damage than individual enzymes at the higher concentration it was chosen for the following studies.

3.4. Inter-individual variation in BLM:Fe(II)-induced DNA damage

Next PBMCs from ten healthy individuals with normal blood counts were tested at two different BLM:Fe(II) concentrations and compared to the untreated PBMCs from the same individual (Fig. 4), using the whole enzyme cocktail. Firstly, we observed a variation in the detected level of damage in the untreated samples of the different individuals ranging from ~6 to ~22 Dots/Mbp, an almost four-fold difference in background levels of DNA-damage (Fig. 4A). To compare the BLM:Fe(II) induced damage in different individuals, the quantified damage in the untreated sample was first subtracted from the value obtained for the treated sample in the same individual and plotted in Fig. 4B. We observed a variation in the BLM:Fe(II) induced damage at both 2 μM and 3 μM with a coefficient of variation (CV) of 75.8 % and 58.2 % respectively. There was an ~8-fold difference between the highest and lowest level of detected damage at 2 μM and ~5-fold at 3 μM. Additionally, the relative ratio of damage between 2 μM and 3 μM varied from ~1.0 to ~10.0.

3.5. Inter-individual variation in repair kinetics for BLM:Fe(II) induced DNA damage

In addition to the level of DNA damage induced in patient cells, the rate at which this damage is repaired is of importance for evaluation of sensitivity to DNA damaging chemotherapy. To investigate the kinetics for repairing BLM:Fe(II)-induced DNA damage, the level of detected damage over time was followed after removal of BLM:Fe(II) (Figs. 5 and S3). Interestingly, we observed a peak level of damage at 20 min post removal of BLM:Fe(II). For three individuals the detected damage was back to background level (untreated sample) at 60 min, indicating complete repair, while for individual 12 this was observed at 90 min, indicating slower repair.

3.6. Detection of DNA repair deficiency in BLM:Fe(II) treated cells

To investigate the ability of the assay in detecting cellular DNA repair deficiencies, PBMCs from two healthy individuals were pre-treated with CRT0044876, a potent APE1 inhibitor [40]. CRT0044876 treatment alone (200 μM) did not affect the amount of damage detected (Fig. 6A-B). However, preincubation of the samples with CRT0044876 for 2 h before treatment with BLM:Fe(II) (2 or 3 μM), led to an increase in damage, compared to BLM:Fe(II) alone in both individuals. The effect is also evident in DNA repair where the damage was completely repaired without CRT0044876 present, but approximately 40–50 % of the damage remained at 90 min in individual 17 and 18 when the cells were preincubated with CRT0044876 for 2 h (Fig. 6C-D).

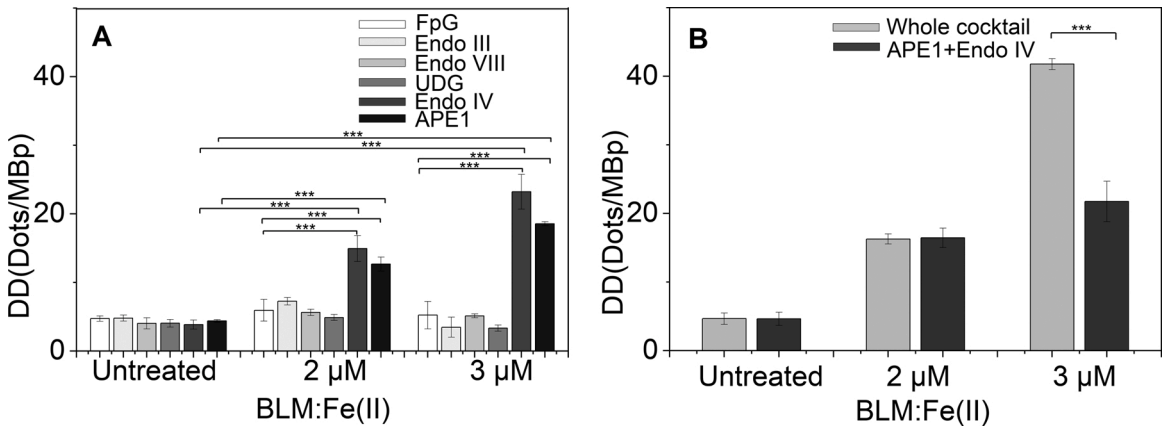

Fig. 3. A. Detected DNA damage (DD) in untreated, BLM:Fe(II)(2 μM) and BLM:Fe(II)(3 μM) treated PBMCs from pooled blood (five healthy individuals), and incubated with single BER enzymes. **B**. DD in untreated, BLM:Fe(II)(2 μM) and BLM:Fe(II)(3 μM) treated PBMCs from pooled blood (five healthy individuals), and incubated with either the whole enzyme cocktail or only APE1 and EndoIV. Error bars indicate the standard deviation from technical triplicates.

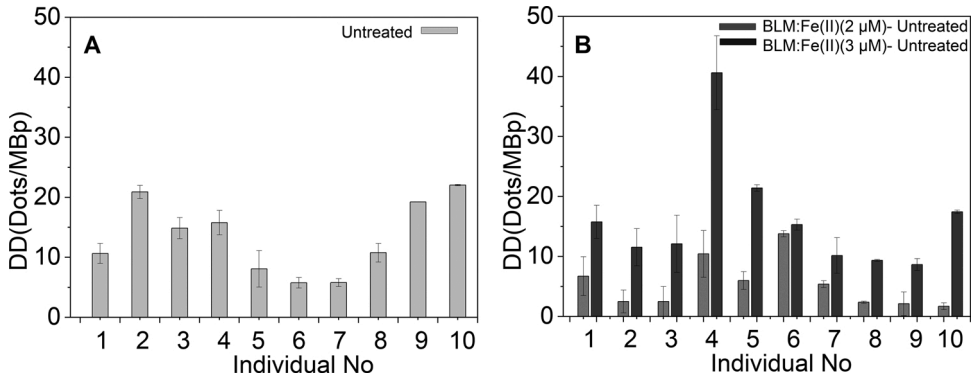

Fig. 4. **A**. Detected DNA damage (DD) in untreated PBMCs from ten healthy individuals. **B**. DD (treated) - DD (untreated) for the same ten healthy individuals at two BLM:Fe(II) concentrations (2 μM or 3 μM). Error bars indicate the standard deviation from technical triplicates (Individual no 1-7) and technical duplicates (Individual no 8-10).

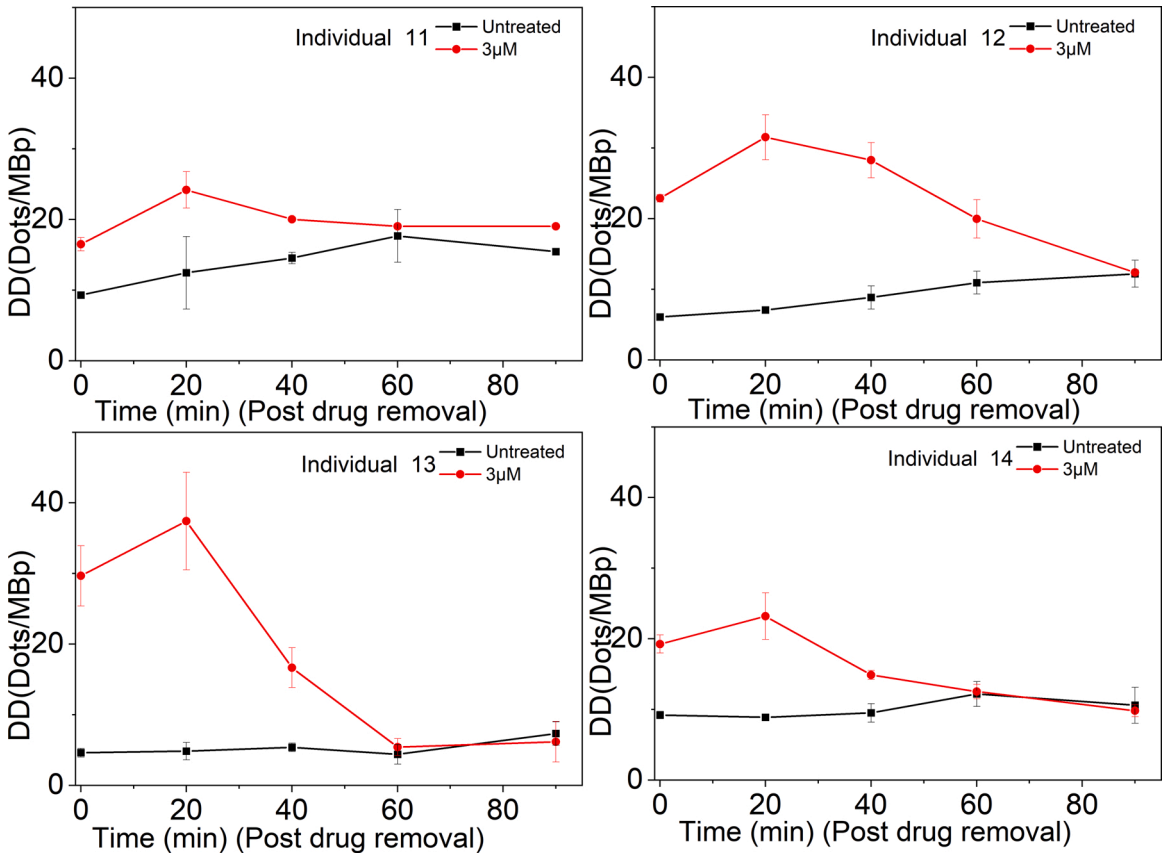

Fig. 5. DNA repair post BLM-Fe(II) treatment (red line) of PBMCs from four healthy individuals exposed to BLM:Fe(II) (3 μM) for 1 h and then incubated in drug-free medium for 0-90 min. The black solid line represents untreated samples followed overtime in similar reaction conditions as BLM:Fe(II) treated samples. Error bars indicate standard deviation calculated from technical duplicates (Individual no 11) and technical triplicates (Individual no 12-14).

4. Discussion

Here, we present an assay based on imaging of single DNA molecules, to quantify global levels of DNA damage caused by BLM in PBMCs prepared from blood samples. PBMCs are a useful source of cells for clinical applications as blood collection is relatively low invasive [41]. Approximately, 70−90% of PBMCs prepared from individuals with a normal blood count are T lymphocytes that are physiologically non-dividing [42,43]. This provides us with a relatively homogenous cell population allowing investigation of inter-individual variation. The DNA damaging activity of BLM is dependent on the metal ion bound to it. While Fe(II) increased the damaging efficiency of BLM, Cu(II) appeared to inhibit its activity. BLM-Fe(II) and oxygen can form an active intermediate, BLM-Fe(III)-O_2^{2-}, that causes strand breaks in DNA [44]. It has been reported that BLM-Cu(II) might dissociate in cells to release free BLM and that this free BLM can take up Fe(II) and cause damages in cells [45]. However, we did not observe any increased damage in our experiments.

The majority of the damage caused by BLM and BLM:Fe(II) could be processed by the apurinic/apyrimidinic (AP) endonucleases APE1 and Endo IV together with DNA polymerase 1, indicating the formation of AP sites, as reported by others [46]. This agrees with previous reports that Endo IV is mainly responsible for processing damages caused by BLM [47] and our study suggests that APE1 also can process BLM-induced

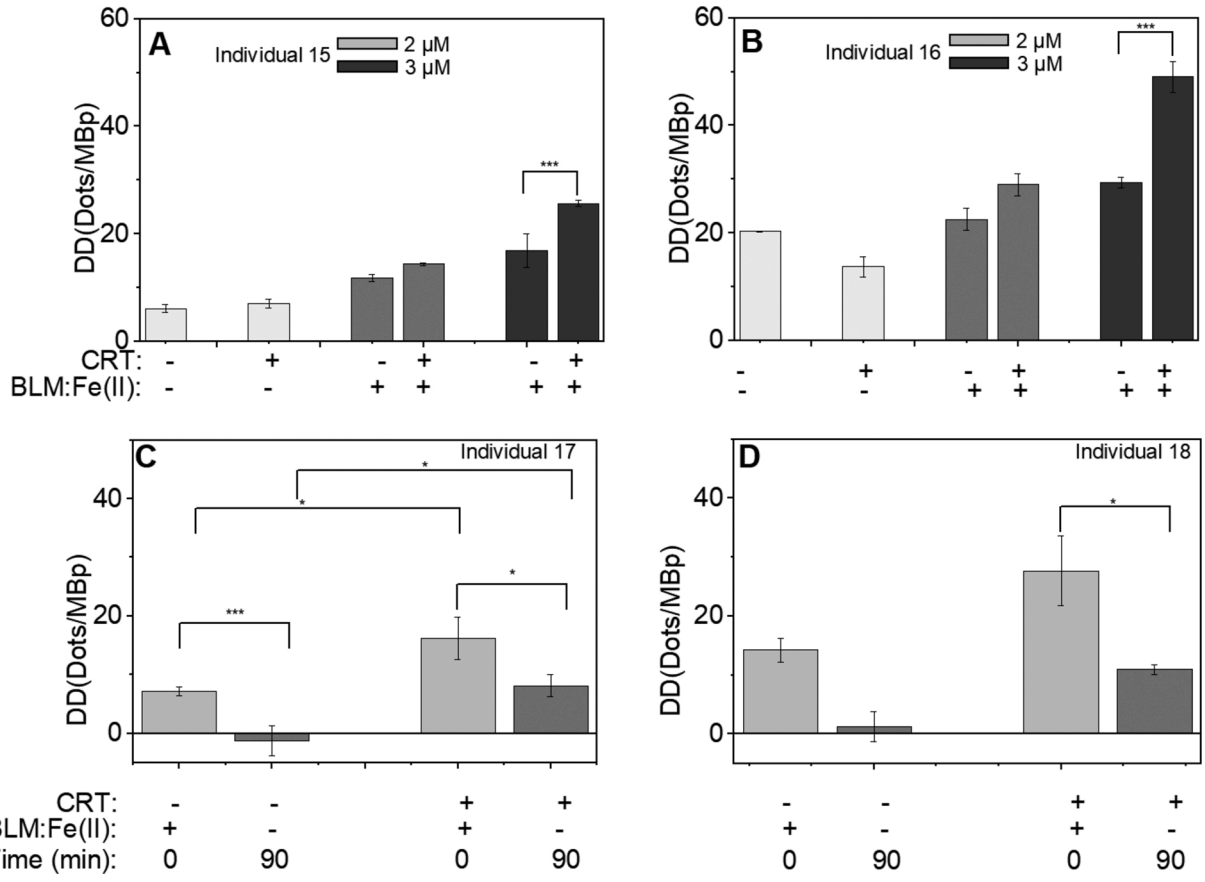

Fig. 6. Detected damage (DD) for PBMCs from healthy individual 15 (**A**) and 16 (**B**) pretreated with/without CRT0044876 (2 h) and BLM:Fe(II) (1 h incubation). Error bars indicate the standard deviation calculated from technical triplicate (Individual no 15) and technical duplicate (Individual no 16). **C**-**D** Detected damage (DD) at 0 and 90 min (post-drug removal) in PBMCs from individual 17 and individual 18 with or without CRT0044876 (200 μM) in presence of BLM:Fe(II) (3 μM) (1 h incubation). Error bars indicate the standard deviation calculated from technical triplicate (Individual no 17) and technical duplicate (Individual no 18).

DNA damage [21,48]. At high levels of BLM:Fe(II) (3 μM), we observed that other repair enzymes included in the cocktail were contributing to the detection of damage. This is likely due to the additional types of oxidative base damages such as 8-OH-Gua, FapyGua, and 5-OH-MeUra that can be caused by BLM [49] at higher concentrations, in addition to the abasic sites.

When the damage induced by BLM in PBMCs from ten individuals was assayed, we observed a variation in several aspects of cellular response. Interestingly, we observed different levels of background damage in the untreated samples. Different levels of intrinsic DNA damage can be an *in vitro* artefact but can be also attributed to for example differences in metabolism, age, genetic disorders *etc*. [50–52]. Our assay also demonstrated inter-individual differences in the damage levels induced by BLM. We observed different levels of damage induction compared to background levels and a variation in the pattern of dose-dependent damage induction. The inter-individual variation may be due to differences in the DNA repair proteins present in the cell, differences in the interaction of the drug with the cell content as well as metabolic differences. For example, in an *in vitro* assay, around ten-fold variation in the activity of MGMT and a two-fold interindividual variation in activity of 8-oxoguanine DNA glycosylase (OGG1) was observed [53–55]. The cell metabolism also affects the DNA repair, for example the amount of methyl and ethyl group donors, metabolic intermediates, nucleotide pools and glutathione [56]. The data indicate that the assay may be used as a tool to monitor the activity of BLM in patient cells.

The assay can also be used to study BLM-induced DNA repair *in vitro*. If the individual *in vitro* damage response and repair observed by the assay is shown to correlate with clinical response in terms of side-effects caused by the drug, we foresee that the assay could potentially be used as a tool in detecting patients that are hypersensitive to BLM prior to treatment. When the rate of DNA damage change was assayed after BLM removal, higher damage levels were observed after 20 min than directly after treatment. There can be two possible reasons for this phenomenon. One possibility is continued formation of strand breaks even after BLM removal, and the other is the occurrence of a transient phase in which damage levels increase due to processing of the damage inside the cells. Some BER intermediates formed during repair can be more toxic than the original damage and these might be detected by the assay [57]. Again, we observed differences in the rate of repair between individuals, highlighting the inter-individual variability in the damage response and the importance of developing assays that detect these differences.

A long-term goal is to use the assay to detect patients with deficiencies in DNA repair, and hence are particularly sensitive to specific chemotherapy drugs and potentially even reveal the molecular mechanism behind this sensitivity. Here the assay detected the DNA repair deficiency in cells pre-incubated with the APE1 inhibitor CRT0044876 [58,59]. It is interesting to note that in both the individuals a large fraction of damage was repaired even in presence of 200 μM of CRT0044876. This might be attributed to CRT0044876 not being able to inhibit APE1 fully as well as the possibility of a compensatory repair pathway [59,60]. However, this study needs to be followed in human cohorts as different individuals can show varying repair profiles.

Our assay can be optimized for other DNA damaging agents, BER pathway inhibitors and other sensitizers for cancer therapy. In the case of BLM, most of the damage was detected by APE1 or Endo IV, but we included also other BER enzymes for an improved detection efficiency. For each new drug to be analyzed, the composition of the enzyme cocktail needs to be optimized.

Funding

This work was funded by grants from Swedish Cancer Society [2017/654 to F.W., 2017/600 O.H.], Swedish Childhood Cancer Foundation [MT2016-0004 and PR2019-0037 to F.W.], EU Horizon 2020 program BeyondSeq [634890 to F.W.], IngaBritt och Arne Lundbergs Forskningsstiftelse [to F.W.], the Swedish Heart and Lung Foundation [to O.H.], the Assar Gabrielsson Cancer Research Foundation [to V.S. and P.J.], and LUA/ALF funding at Sahlgrenska University Hospital [to O.H.].

CRediT authorship contribution statement

Vandana Singh: Conceptualization, Methodology, Validation, Formal analysis, Investigation, Writing - original draft, Funding acquisition. **Pegah Johansson:** Conceptualization, Resources, Writing - review & editing, Supervision. **Yii-Lih Lin:** Software. **Ola Hammarsten:** Conceptualization, Resources, Writing - review & editing, Supervision, Funding acquisition. **Fredrik Westerlund:** Conceptualization, Methodology, Writing - review & editing, Supervision, Project administration, Funding acquisition.

Declaration of competing interest

The authors declare that they have no known competing financial interests or personal relationships that could have appeared to influence the work reported in this paper.

Acknowledgements

The authors would like to acknowledge the hematology staff at the Department of Clinical Chemistry at Sahlgrenska University Hospital for providing blood samples. The analysis software was developed by the group of Prof. Yuval Ebenstein at Tel Aviv University. We acknowledge Prof. Yuval Ebenstein for fruitful discussions.

Appendix A. Supplementary data

Supplementary material related to this article can be found, in the online version, at doi:https://doi.org/10.1016/j.dnarep.2021.103153.

References

[1] J. Zhang, Z. Zheng, M. Wu, L. Zhang, J. Wang, W. Fu, N. Xu, Z. Zhao, Y. Lao, H. Xu, The natural compound neobractatin inhibits tumor metastasis by upregulating the RNA-binding-protein MBNL2, Cell Death Dis. 10 (2019) 554.
[2] H. Uga, C. Kuramori, A. Ohta, Y. Tsuboi, H. Tanaka, M. Hatakeyama, Y. Yamaguchi, T. Takahashi, M. Kizaki, H. Handa, A new mechanism of methotrexate action revealed by target screening with affinity beads, Mol. Pharmacol. 70 (2006) 1832–1839.
[3] D.A. Skoufias, L. Wilson, Mechanism of inhibition of microtubule polymerization by colchicine: inhibitory potencies of unliganded colchicine and tubulin-colchicine complexes, Biochemistry 31 (1992) 738–746.
[4] L.H. Swift, R.M. Golsteyn, Genotoxic anti-cancer agents and their relationship to DNA damage, mitosis, and checkpoint adaptation in proliferating cancer cells, Int. J. Mol. Sci. 15 (2014) 3403–3431.
[5] J. Lokich, N. Anderson, Carboplatin versus cisplatin in solid tumors: an analysis of the literature, Ann. Oncol. 9 (1998) 13–21.
[6] B.S. Andersson, A. Kashyap, V. Gian, J.R. Wingard, H. Fernandez, P.J. Cagnoni, R. B. Jones, S. Tarantolo, W.W. Hu, K.G. Blume, S.J. Forman, R.E. Champlin, Conditioning therapy with intravenous busulfan and cyclophosphamide (IV BuCy2) for hematologic malignancies prior to allogeneic stem cell transplantation: a phase II study, Biol. Blood Marrow Transplant. 8 (2002) 145–154.
[7] C. Bailly, A. Kénani, M.J. Waring, Altered cleavage of DNA sequences by bleomycin and its deglycosylated derivative in the presence of actinomycin, Nucleic Acids Res. 25 (1997) 1516–1522.
[8] K. Tecza, J. Pamula-Pilat, J. Lanuszewska, D. Butkiewicz, E. Grzybowska, Pharmacogenetics of toxicity of 5-fluorouracil, doxorubicin and cyclophosphamide chemotherapy in breast cancer patients, Oncotarget 9 (2018) 9114–9136.
[9] J.B. Schwartz, The current state of knowledge on age, sex, and their interactions on clinical pharmacology, Clin. Pharmacol. Ther. 82 (2007) 87–96.
[10] H. Umezawa, K. Maeda, T. Takeuchi, Y. Okami, New antibiotics, bleomycin A and B, J. Antibiot. (Tokyo) 19 (1966) 200–209.
[11] T.M. Karpiński, A. Adamczak, Anticancer activity of bacterial proteins and peptides, Pharmaceutics 10 (2018).
[12] R.M. Burger, J. Peisach, S.B. Horwitz, Activated bleomycin. A transient complex of drug, iron, and oxygen that degrades DNA, J. Biol. Chem. 256 (1981) 11636–11644.
[13] E.A. Sausville, J. Peisach, S.B. Horwitz, Effect of chelating agents and metal ions on the degradation of DNA by bleomycin, Biochemistry 17 (1978) 2740–2746.
[14] E.A. Rao, L.A. Saryan, W.E. Antholine, D.H. Petering, Cytotoxic and antitumor properties of bleomycin and several of its metal complexes, J. Med. Chem. 23 (1980) 1310–1318.
[15] K. Nagai, H. Yamaki, H. Suzuki, N. Tanaka, H. Umezawa, The combined effects of bleomycin and sulfhydryl compounds on the thermal denaturation of DNA, Biochim. Biophys. Acta 179 (1969) 165–171.
[16] S.M. Hecht, Bleomycin: new perspectives on the mechanism of action, J. Nat. Prod. 63 (2000) 158–168.
[17] L.F. Povirk, Y.H. Han, R.J. Steighner, Structure of bleomycin-induced DNA double-strand breaks: predominance of blunt ends and single-base 5' extensions, Biochemistry 28 (1989) 5808–5814.
[18] A.M. Whitaker, T.S. Flynn, B.D. Freudenthal, Molecular snapshots of APE1 proofreading mismatches and removing DNA damage, Nat. Commun. 9 (2018) 399.
[19] S.H. Wilson, T.A. Kunkel, Passing the baton in base excision repair, Nat. Struct. Biol. 7 (2000) 176–178.
[20] V. Singh, P. Das, Condensation of DNA–a putative obstruction for repair process in abasic clustered DNA damage, DNA Repair (Amst.) 12 (2013) 450–457.
[21] V. Singh, B. Kumari, P. Das, Repair efficiency of clustered abasic sites by APE1 in nucleosome core particles is sequence and position dependent, RSC Adv. 5 (2015).
[22] M.Z. Mohammed, V.N. Vyjayanti, C.A. Laughton, L.V. Dekker, P.M. Fischer, D. M. Wilson, R. Abbotts, S. Shah, P.M. Patel, I.D. Hickson, S. Madhusudan, Development and evaluation of human AP endonuclease inhibitors in melanoma and glioma cell lines, Br. J. Cancer 104 (2011) 653–663.
[23] L. Liu, S.L. Gerson, Therapeutic impact of methoxyamine: blocking repair of abasic sites in the base excision repair pathway, Curr. Opin. Investig. Drugs 5 (2004) 623–627.
[24] A.R. Collins, The comet assay for DNA damage and repair: principles, applications, and limitations, Mol. Biotechnol. 26 (2004) 249–261.
[25] I.J. Chopra, D.H. Solomon, G.N. Beall, Radioimmunoassay for measurement of triiodothyronine in human serum, J. Clin. Invest. 50 (1971) 2033–2041.
[26] G. Figueroa-González, C. Pérez-Plasencia, Strategies for the evaluation of DNA damage and repair mechanisms in cancer, Oncol. Lett. 13 (2017) 3982–3988.
[27] T.R. Berton, D.L. Mitchell, Quantification of DNA photoproducts in mammalian cell DNA using radioimmunoassay, Methods Mol. Biol. 920 (2012) 177–187.
[28] M.S. Cooke, R. Olinski, S. Loft, European Standards Committee on Urinary (DNA) Lesion Analysis, Measurement and meaning of oxidatively modified DNA lesions in urine, Cancer Epidemiol. Biomarkers Prev. 17 (2008) 3–14.
[29] K. Boguszewska, M. Szewczuk, S. Urbaniak, B.T. Karwowski, Review: immunoassays in DNA damage and instability detection, Cell. Mol. Life Sci. 76 (2019) 4689–4704.
[30] J. Lee, H.S. Park, S. Lim, K. Jo, Visualization of UV-induced damage on single DNA molecules, Chem. Commun. (Camb.) 49 (2013) 4740–4742.
[31] J. Lee, Y. Kim, S. Lim, K. Jo, Single-molecule visualization of ROS-induced DNA damage in large DNA molecules, Analyst 141 (2016) 847–852.
[32] S. Zirkin, S. Fishman, H. Sharim, Y. Michaeli, J. Don, Y. Ebenstein, Lighting up individual DNA damage sites by in vitro repair synthesis, J. Am. Chem. Soc. 136 (2014) 7771–7776.
[33] I. Obi, M. Rentoft, V. Singh, J. Jamroskovic, K. Chand, E. Chorell, F. Westerlund, N. Sabouri, Stabilization of G-quadruplex DNA structures in Schizosaccharomyces pombe causes single-strand DNA lesions and impedes DNA replication, Nucleic Acids Res. 48 (19) (2020) 10998–11015.
[34] D. Torchinsky, Y. Michaeli, N.R. Gassman, Y. Ebenstein, Simultaneous detection of multiple DNA damage types by multi-colour fluorescent labelling, Chem. Commun. (Camb.) 55 (2019) 11414–11417.
[35] N.W. Holton, Y. Ebenstein, N.R. Gassman, Broad spectrum detection of DNA damage by repair assisted damage detection (RADD), DNA Repair (Amst.) 66-67 (2018) 42–49.
[36] V. Müller, A. Dvirnas, J. Andersson, V. Singh, S. Kk, P. Johansson, Y. Ebenstein, T. Ambjörnsson, F. Westerlund, Enzyme-free optical DNA mapping of the human genome using competitive binding, Nucleic Acids Res. 47 (15) (2019) e89.
[37] V. Singh, P. Johansson, D. Torchinsky, Y.L. Lin, R. Oz, Y. Ebenstein, O. Hammarsten, F. Westerlund, Quantifying DNA damage induced by ionizing radiation and hyperthermia using single DNA molecule imaging, Transl. Oncol. 13 (2020), 100822.
[38] Q. Wei, W. Luo, S. Chiang, T. Kappel, C. Mejia, D. Tseng, R.Y. Chan, E. Yan, H. Qi, F. Shabbir, H. Ozkan, S. Feng, A. Ozcan, Imaging and sizing of single DNA molecules on a mobile phone, ACS Nano 8 (2014) 12725–12733.
[39] N. Gilat, T. Tabachnik, A. Shwartz, T. Shahal, D. Torchinsky, Y. Michaeli, G. Nifker, S. Zirkin, Y. Ebenstein, Single-molecule quantification of 5-hydroxymethylcytosine for diagnosis of blood and colon cancers, Clin. Epigenetics 9 (2017) 70.
[40] S. Madhusudan, F. Smart, P. Shrimpton, J.L. Parsons, L. Gardiner, S. Houlbrook, D. C. Talbot, T. Hammonds, P.A. Freemont, M.J. Sternberg, G.L. Dianov, I.D. Hickson, Isolation of a small molecule inhibitor of DNA base excision repair, Nucleic Acids Res. 33 (2005) 4711–4724.
[41] N.L. Anderson, N.G. Anderson, The human plasma proteome: history, character, and diagnostic prospects, Mol. Cell Proteomics 1 (2002) 845–867.

[42] H.L. Cooper, S.L. Berger, R. Braverman, Free ribosomes in physiologically nondividing cells. Human peripheral lymphocytes, J. Biol. Chem. 251 (1976) 4891–4900.
[43] G.P. Dorneles, I.M. da Silva, M.A. Santos, V.R. Elsner, S.G. Fonseca, A. Peres, P.R. T. Romão, Immunoregulation induced by autologous serum collected after acute exercise in obese men: a randomized cross-over trial, Sci. Rep. 10 (2020) 21735.
[44] H. Kuramochi, K. Takahashi, T. Takita, H. Umezawa, An active intermediate formed in the reaction of bleomycin-Fe(II) complex with oxygen, J. Antibiot. (Tokyo) 34 (1981) 576–582.
[45] W.E. Antholine, D. Solaiman, L.A. Saryan, D.H. Petering, Studies on the chemical reactivity of copper bleomycin, J. Inorg. Biochem. 17 (1982) 75–94.
[46] L.F. Povirk, DNA damage and mutagenesis by radiomimetic DNA-cleaving agents: bleomycin, neocarzinostatin and other enediynes, Mutat. Res. 355 (1996) 71–89.
[47] D.O. Onyango, A. Naguleswaran, S. Delaplane, A. Reed, M.R. Kelley, M. M. Georgiadis, W.J. Sullivan, Base excision repair apurinic/apyrimidinic endonucleases in apicomplexan parasite Toxoplasma gondii, DNA Repair (Amst.) 10 (2011) 466–475.
[48] J.D. Levin, B. Demple, In vitro detection of endonuclease IV-specific DNA damage formed by bleomycin in vivo, Nucleic Acids Res. 24 (1996) 885–889.
[49] D.H. Atha, E. Coskun, O. Erdem, A. Tona, V. Reipa, B.C. Nelson, Genotoxic effects of etoposide, bleomycin, and ethyl methanesulfonate on cultured CHO cells: analysis by GC-MS/MS and comet assay, J. Nucleic Acids 2020 (2020), 8810105.
[50] J.H. Hoeijmakers, DNA damage, aging, and cancer, N. Engl. J. Med. 361 (2009) 1475–1485.
[51] H. Atamna, I. Cheung, B.N. Ames, A method for detecting abasic sites in living cells: age-dependent changes in base excision repair, Proc. Natl. Acad. Sci. U. S. A. 97 (2000) 686–691.
[52] E.M. Sturgis, R. Zheng, L. Li, E.J. Castillo, S.A. Eicher, M. Chen, S.S. Strom, M. R. Spitz, Q. Wei, XPD/ERCC2 polymorphisms and risk of head and neck cancer: a case-control analysis, Carcinogenesis 21 (2000) 2219–2223.
[53] P.N. O'Donnell, P.V. Barber, G.P. Margison, A.C. Povey, Association between O6-alkylguanine-DNA-alkyltransferase activity in peripheral blood lymphocytes and bronchial epithelial cells, Cancer Epidemiol. Biomarkers Prev. 8 (1999) 641–645.
[54] B. Myrnes, K.E. Giercksky, H. Krokan, Interindividual variation in the activity of O6-methyl guanine-DNA methyltransferase and uracil-DNA glycosylase in human organs, Carcinogenesis 4 (1983) 1565–1568.
[55] K. Janssen, K. Schlink, W. Götte, B. Hippler, B. Kaina, F. Oesch, DNA repair activity of 8-oxoguanine DNA glycosylase 1 (OGG1) in human lymphocytes is not dependent on genetic polymorphism Ser326/Cys326, Mutat. Res. 486 (2001) 207–216.
[56] M.O. Turgeon, N.J.S. Perry, G. Poulogiannis, DNA damage, repair, and cancer metabolism, Front. Oncol. 8 (2018) 15.
[57] Y.J. Kim, D.M. Wilson, Overview of base excision repair biochemistry, Curr. Mol. Pharmacol. 5 (2012) 3–13.
[58] A. Schäfer, L. Schomacher, G. Barreto, G. Döderlein, C. Niehrs, Gemcitabine functions epigenetically by inhibiting repair mediated DNA demethylation, PLoS One 5 (2010), e14060.
[59] L.P. Franchi, J.E.B. de Freitas Lima, H.L. Piva, A.C. Tedesco, The redox function of apurinic/apyrimidinic endonuclease 1 as key modulator in photodynamic therapy, J. Photochem. Photobiol. B 211 (2020), 111992.
[60] S. Boiteux, M. Guillet, Abasic sites in DNA: repair and biological consequences in Saccharomyces cerevisiae, DNA Repair (Amst.) 3 (2004) 1–12.